

# Design Criteria of X-wave Launchers for Millimeter-Wave Applications

Walter Fuscaldo\*, Santi C. Pavone†, Davide Comite\*,

Guido Valerio‡, Matteo Albani†, Mauro Ettore§, and Alessandro Galli\*

\* Department of Information Engineering, Electronics and Telecommunications (DIET)

Sapienza University of Rome, 00184 Rome, Italy.

Email: fuscaldo@diet.uniroma1.it

† Department of Information Engineering and Mathematics (DIISM)

University of Siena, 53100 Siena, Italy.

‡ Sorbonne Universités, UPMC Univ Paris 06, UR2, L2E, Paris, France.

§ Institut d'Électronique et de Télécommunications de Rennes (IETR), UMR CNRS 6164

Université de Rennes 1, 35042 Rennes, France.

**Abstract**—Bessel-beam launchers are promising and established technologies for focusing applications at microwaves. Their use in time-domain leads to the definition of a new class of devices, viz., the X-wave launchers, that are currently under theoretical investigation. In this work, we discuss the focusing features of such devices with a specific interest at millimeter waves. By reviewing the mathematical expressions that describe the spatial resolutions of these systems, we establish here novel operating conditions which might be particularly appealing for specific millimeter-wave applications. In addition, alternative criteria for designing X-wave launchers are derived, showing that an electrically-large aperture is not strictly required, as it seemed from previous works. However, it is shown that the use of an electrically-small aperture would demand a considerably wideband capability. The various discussions as well as the additional degrees of freedom presented here furnish useful informations which might help the application-oriented design of X-wave launchers in the microwave/millimeter-wave range.

**Index Terms**— Bessel beams, X-waves, nondiffracting waves, localized waves, millimeter waves.

## I. INTRODUCTION

In applications such as security screening, medical imaging, and radiometry, to name but a few, it is important to focus the energy in the millimeter-wave range to benefit of both the non-ionizing character of millimeter waves and their millimeter resolution.

In this context, nondiffracting waves [1], especially Bessel beams and their polychromatic version, i.e., X-waves, are gaining increasing attention in the millimeter-wave community due to their remarkable focusing features [2].

Bessel beams [3] as well as X-waves [4] are able to maintain their nondiffractive character along the propagating axis for a large distance (commonly known as *nondiffractive range*) as experimentally demonstrated in optics and acoustics (see [1] and Refs. therein). Interestingly, while Bessel beams are focused only along the transverse axis (being their transverse section almost invariant along the longitudinal axis), X-waves are focused along both the transverse and the longitudinal axis (see Fig. 1).

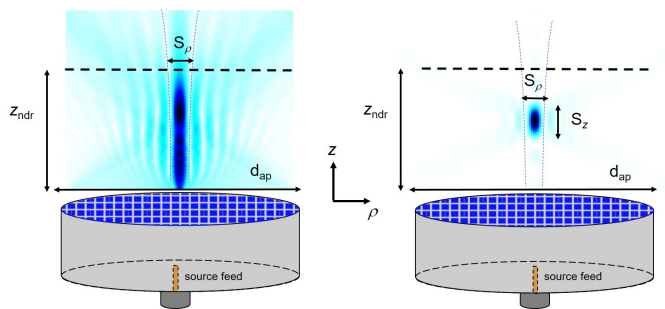


Fig. 1. Comparison between Bessel-beam launchers and X-wave launchers. On the left-side, a Bessel-beam launcher generating a transversely focused Bessel beam with transverse spot size  $S_\rho$ . The transverse profile is maintained along the longitudinal axis up to the nondiffractive range  $z_{\text{ndr}}$ . On the right side, the same device acts as an X-wave launcher in the time domain. The propagation of a focused X-wave is captured at a given time instant. Differently from the Bessel beam, the X-wave is confined also along the longitudinal  $z$ -axis where it exhibits a longitudinal spot size  $S_z$  considerably narrower than  $z_{\text{ndr}}$ .

Unfortunately, even if Bessel beams have been experimentally generated in the microwave and millimeter-wave range (see, e.g., [5], [6]), experimental results for X-waves are still lacking, except for some very preliminary results [7]. The reason for this temporary lack has been recently motivated in [4], where the development of an original theoretical framework has allowed the derivation of several physical insights on the problem. The proposed analysis revealed that the design of an *efficient* X-wave launcher (i.e., able to focus energy along both the transverse and the longitudinal axis) usually requires a moderate wavenumber dispersion, a wide fractional bandwidth, and an electrically-large aperture. These requirements actually limit the class of suitable devices at millimeter waves, even if some preliminary designs have already been proposed [4], [7], [8]. In such works, the design process takes advantage of the concept of metric of confinement introduced in [4].

In this work, we provide a more general criterion for designing X-wave launchers showing that an electrically-large

aperture is not theoretically required to focus energy along both directions. Using the results recently outlined in [9], we show that the aperture size reduction dictates a larger fractional bandwidth.

The paper is organized as follows. In Section I, the focusing features of X-waves are briefly outlined. In Section II, we review the concept of metric of confinement and discuss some original aspects which might be particularly relevant for specific millimeter-wave applications. In Section III the criteria for designing electrically-small apertures are discussed. Finally, conclusions are drawn.

## II. NONDIFFRACTIVE FEATURES OF X-WAVES

X-waves can be obtained as a spectral superposition of Bessel beams with the same *axicon angle* [1] over a certain frequency bandwidth  $\Delta\omega$  (throughout the paper, we consider only *spectrally-flat* X-waves, i.e., we tacitly assume a uniform frequency spectrum):

$$\chi(\rho, z, t) = \int_{\Delta\omega} J_0(k_\rho(\omega)\rho) e^{-jk_z(\omega)z} e^{j\omega t} d\omega, \quad (1)$$

where  $J_0(\cdot)$  is a zeroth-order Bessel function of the first kind,  $\omega$  is the angular frequency,  $t$  is time,  $k_\rho$  and  $k_z$  are the wavenumbers along the radial  $\rho$  and longitudinal  $z$  directions, respectively (in turn related each other through the separation relation  $k_0^2 = k_\rho^2 + k_z^2$ , where  $k_0$  is the free-space wavenumber), and  $\theta = \arctan[k_\rho(\omega)/k_z(\omega)]$  is the axicon angle. Therefore, any Bessel-beam launcher characterized by a negligible wavenumber dispersion over a certain frequency bandwidth is able to act as an X-wave launcher in time domain. Moreover, since X-waves are obtained from Bessel beams, they inherit their focusing features.

Specifically, X-waves are localized along the transverse axis and maintain their transverse spot size  $S_\rho$  up to the nondiffractive range  $z_{\text{ndr}} = \rho_{\text{ap}} \cot \theta$  [3], where  $\rho_{\text{ap}} = d_{\text{ap}}/2$  is the aperture radius. In addition, X-waves are also localized along the longitudinal propagating axis. However, the longitudinal spot size  $S_z$  is narrow as long as a considerable fractional bandwidth is guaranteed [4]. This results from the definition of a suitable metric of confinement for X-waves [4], [9], as we will review in the following paragraphs.

### A. Metric of confinement

The definition of metric of confinement states that X-waves are localized if and only if both their transverse  $S_\rho$  and longitudinal  $S_z$  spot sizes are smaller than the aperture diameter  $d_{\text{ap}}$  and the nondiffractive range  $z_{\text{ndr}}$ , respectively [4], [9]. Hence, by introducing the following confinement ratios

$$C_\rho = S_\rho/d_{\text{ap}}, \quad (2)$$

$$C_z = S_z/z_{\text{ndr}} \quad (3)$$

the definition of the following metric of confinement is straightforward:

$$C_{\rho,z} = \begin{cases} 1 & \text{if } \max(C_\rho, C_z) > 1, \\ C_\rho C_z & \text{elsewhere,} \end{cases} \quad (4)$$

Clearly, when  $C_{\rho,z} < 1$ , the resulting X-wave will be confined along *both* the radial *and* the longitudinal direction and the value of  $C_{\rho,z}$  gives a well-defined measure of the localization of the energy. Otherwise, when  $C_{\rho,z} = 1$  the X-wave would not be confined along the radial *or* the longitudinal direction.

### B. Resolutions along the radial and longitudinal axis

For *spectrally flat* X-waves, the expressions for  $S_\rho$  and  $S_z$  and in turn  $C_\rho$  and  $C_z$  are given in analytical closed form [4]. In the case of a *nondispersive* X-wave characterized by an axicon angle  $\theta$  and generated at the carrier angular frequency  $\omega_0$  around a fractional bandwidth  $\text{FBW} = \Delta\omega/\omega_0$ ,  $S_\rho$  and  $S_z$  take the following expressions:

$$S_\rho = \frac{j_{0,1}\lambda_0}{\pi \sin \theta}, \quad (5)$$

$$S_z = \frac{2\pi\lambda_0}{\text{FBW} \cos \theta}, \quad (6)$$

where  $j_{0,1} \simeq 2.405$  is the first null of the zeroth-order Bessel function of the first kind, and  $\lambda_0 = 2\pi/k_0$ , with  $k_0 = \omega_0/c_0$ . From these expressions, we note that the transverse resolution  $S_\rho$  is lower-bounded by  $\lambda_0/1.3$  (which is close to the Abbe diffraction limit for optical systems [10]), whereas the longitudinal resolution  $S_z$  could, in principle, arbitrarily be reduced by increasing the fractional bandwidth. Nonetheless, millimeter-wave radiating systems operating over more than one octave are unfeasible, thus  $S_z$  is also practically lower-bounded by  $2\pi\lambda_0$ .

It is worth noting here that the axicon angle has an opposite effect over the longitudinal and the transverse resolutions, and thus it is not possible to narrow the resolution along both directions by changing solely the axicon angle.

From the expressions of  $S_\rho$  and  $S_z$ , those of the confinement ratios  $C_\rho$  and  $C_z$  are readily found

$$C_\rho = \frac{j_{0,1}}{(\rho_{\text{ap}}/\lambda_0)2\pi \sin \theta}, \quad (7)$$

$$C_z = \frac{2 \sin \theta}{(\rho_{\text{ap}}/\lambda_0)\text{FBW} \cos^2 \theta}. \quad (8)$$

As for  $S_\rho$  and  $S_z$  it is manifest that the FBW is the only parameter that allows for improving the longitudinal localization without negatively affects the transverse one.

A numerical demonstration of this aspect is reported in Fig. 2. In Figs. 2(a)–(d), the metric of confinement  $C_{\rho,z}$  is reported as a contour-plot of the two variables  $\rho_{\text{ap}}/\lambda_0$  and  $\theta$  for values of  $\text{FBW} = 1\%$ ,  $10\%$ ,  $20\%$ ,  $50\%$ . The black region represents the pairs of values  $(\rho_{\text{ap}}/\lambda_0, \theta)$  for which the X-wave is not confined along at least one direction for a given value of FBW. This region is determined by the intersection of the two boundaries (see blue solid lines) that represent the condition for which  $C_\rho = 1$  (upper boundary) and that for which  $C_z = 1$  (lower boundary), respectively.

As is shown, the region within these two boundaries increases as the FBW increases. In other words, a pair of values  $(\rho_{\text{ap}}/\lambda_0, \theta)$  for which the X-wave is not confined for a certain FBW, might be confined for a higher FBW. This

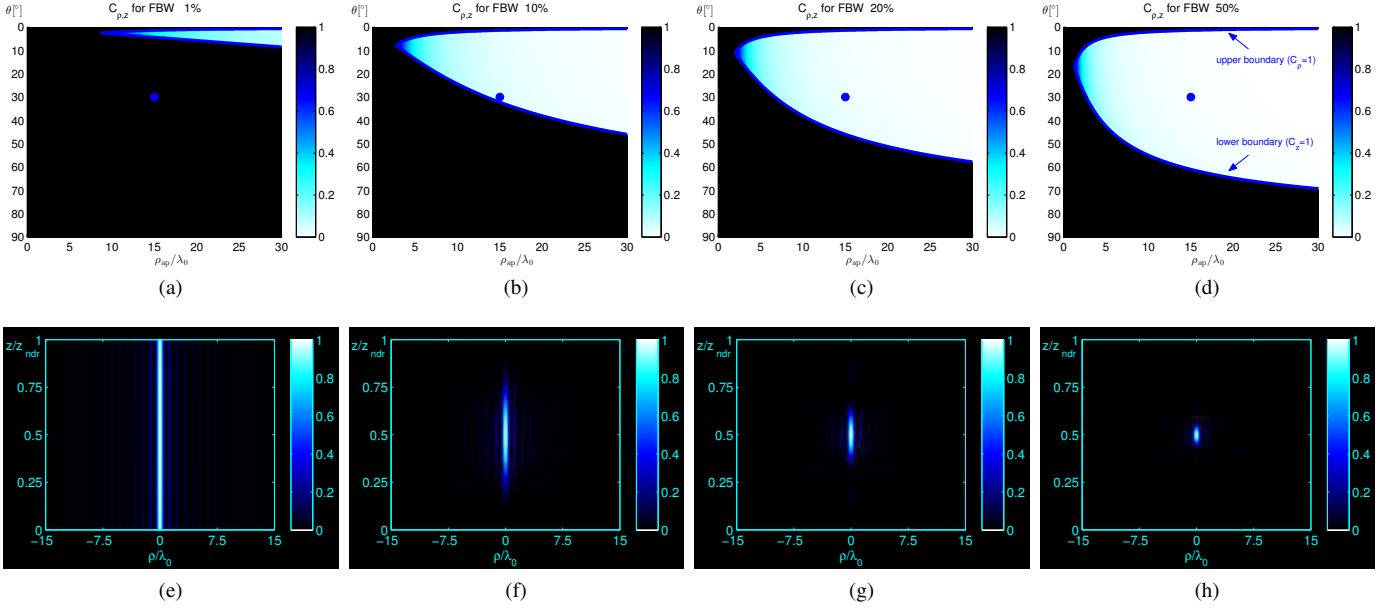


Fig. 2. (a)–(d) The metric of confinement  $C_{\rho,z}$  vs.  $\rho_{\text{ap}}/\lambda_0$  and  $\theta$  is shown for (a) FBW = 1%, (b) FBW = 10%, (c) FBW = 20%, and (d) FBW = 50%. In the black region  $C_\rho > 1$  or  $C_z > 1$ , thus the resulting X-wave is not be confined along *both* axes. The solid blue lines represent the boundaries for which  $C_\rho = 1$  (upper boundary) and  $C_z = 1$  (lower boundary). The two boundaries cross at  $\theta = \theta'_{\text{eq}}$  and  $\rho'_{\text{eq}}$ . (e)–(h) Normalized field intensities  $|\chi(\rho, z, t_0)|^2 / \max |\chi|^2$  vs.  $\rho/\rho_{\text{ap}}$  and  $z/z_{\text{ndr}}$  for an X-wave generated with  $\theta = 30^\circ$  and  $\rho_{\text{ap}} = 15\lambda_0$  (see the blue dots in Figs. 2(a)–(d)). The time  $t$  is set at the instant  $t_0$  the X-wave peak has reached  $z = z_{\text{ndr}}$ .

is corroborated by numerical simulations (see Fig. 2(e)–(f)) considering a non-dispersive X-wave characterized by the pair  $(\rho_{\text{ap}}/\lambda_0 = 15, \theta = 30^\circ)$  (see blue dots in Fig. 2(a)–(d)). As is shown, for low fractional bandwidths the X-wave is loosely localized along the longitudinal axis (the main spot has a ‘needle-like’ shape), whereas it is tightly focused (the main spot has a ‘bullet-like’ shape) for high fractional bandwidths.

### C. Resolution equalization and confinement equalization

For some applications, such as medical imaging, it could be more important to have the same resolution along both axes (i.e.,  $S_\rho = S_z$ ), rather than the narrowest one. Then, it is interesting to find the operating conditions which allow for equalizing the transverse and longitudinal resolutions. By equating the expressions of  $S_\rho$  and  $S_z$ , it is readily found that the equalization condition for resolution is obtained for  $\theta_{\text{eq}}$

$$\theta_{\text{eq}} = \arctan\left(\frac{j_{0,1}\text{FBW}}{2\pi}\right) \simeq \arctan(0.38\text{FBW}) \quad (9)$$

As an example, for a fractional bandwidth of 20% the equalization condition for resolution is achieved at an axicon angle  $\theta_{\text{eq}}$  of approximately  $4^\circ$ , whereas for a fractional bandwidth of 50%, the axicon angle should be approximately  $11^\circ$ .

This criterion furnishes the design rule to equalize the *absolute* resolutions (measured in meters). However, for some other applications, such as wireless power transfer, it could be more interesting to have the same *relative* resolutions (adimensional) with respect to the aperture diameter and the nondiffractive range, for the radial and longitudinal direction, respectively. This can be accomplished by equalizing the

confinement ratios along both axes (i.e.,  $C_\rho = C_z$ ) in place of the resolutions (i.e.,  $S_\rho = S_z$ ). In that case, Eq. (9) should be replaced by

$$\theta'_{\text{eq}} = \arctan\sqrt{\frac{j_{0,1}\text{FBW}}{4\pi}} \simeq \arctan(0.44\sqrt{\text{FBW}}) \quad (10)$$

where  $\theta'_{\text{eq}}$  gives the condition for equalizing the confinements rather than the resolutions.

As an example, for a fractional bandwidth of 20% the equalization condition for confinement is achieved at an axicon angle  $\theta'_{\text{eq}}$  of approximately  $11^\circ$ , whereas for a fractional bandwidth of 50%, the axicon angle should be approximately  $17^\circ$ . These results can also be inferred from Fig. 2(c)–(d). Indeed, the upper and lower boundaries of the metric of confinement (see blue lines in Fig. 2(a)–(d)) meet at  $\theta = \theta'_{\text{eq}}$  and  $\rho_{\text{ap}}/\lambda_0 = \rho'_{\text{eq}}$  with

$$\rho'_{\text{eq}} = j_{0,1}/2\pi \sin \theta'_{\text{eq}}. \quad (11)$$

At this point (viz.,  $(\theta'_{\text{eq}}, \rho'_{\text{eq}})$ ) we clearly have  $C_\rho = C_z = 1$  (which represents the limit condition of non-efficient confinement).

### III. ALTERNATIVE CRITERIA FOR ELECTRICALLY-SMALL APERTURES

In the previous paragraph, we focused on the equalization of the resolutions. Also, from the definitions of the confinement ratios we have understood why X-wave launchers generally require an electrically-large aperture, a considerable fractional bandwidth, and a low axicon angle [4]. In fact, from Figs. 2(a)–(b), it appears that for low fractional bandwidths

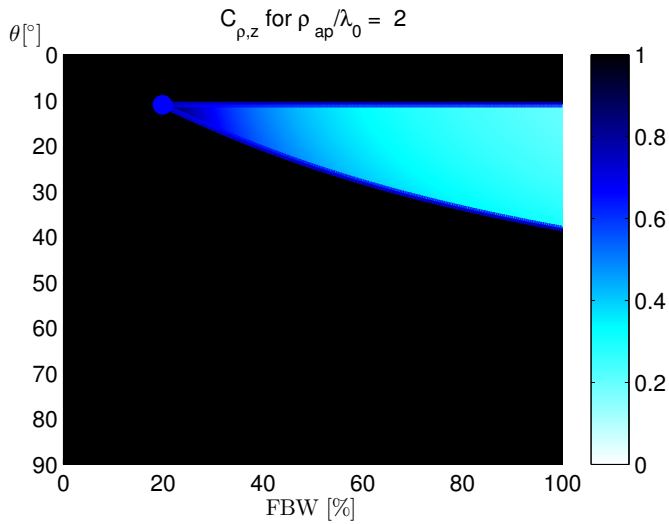


Fig. 3. The metric of confinement  $C_{\rho,z}$  vs. FBW and  $\theta$  is shown for  $\rho_{\text{ap}} = 2\lambda_0$ . The blue solid lines represent the boundaries for which  $C_{\rho} = 1$  and  $C_z = 1$ . The two boundaries cross at  $\text{FBW} = \text{FBW}_{\text{min}}$  and  $\theta = \theta_{\text{min}}$  (see the blue dot).

and electrically-small apertures, an efficient confinement is possible only for few values of the axicon angle around  $10^\circ$ . However, the situation is rather different for higher fractional bandwidths (see Figs. 2(c)–(d)), for which efficient confinement is possible for axicon angles up to  $40^\circ$ .

All these aspects can be recast in a more systematic way, by inspection of Eqs. (7) and (8). In fact, from Eq. (7) one finds that the condition for having a transversely localized X-wave (i.e.,  $C_{\rho} < 1$ ) gives an aperture radius  $\rho_{\text{ap}}/\lambda_0 > 0.38/\sin\theta$ , which is lower-bounded by the value 0.38. This means that, even for such electrically-short apertures, a minimum axicon angle  $\theta_{\text{min}}$  would exist beyond which the X-wave will be transversely confined

$$\theta > \theta_{\text{min}} = \arcsin\left(\frac{j_{0,1}}{2\pi\rho_{\text{ap}}/\lambda_0}\right). \quad (12)$$

However, since the metric of confinement is lower than 1 if and only if the maximum between  $C_{\rho}$  and  $C_z$  is lower than 1 (see Eq. (4)), the X-wave has to be also longitudinally confined (i.e.,  $C_z < 1$ ) at  $\theta_{\text{min}}$ . Then, from Eq. (7), it results that the fractional bandwidth has to be greater than a minimum value  $\text{FBW}_{\text{min}}$

$$\text{FBW} > \text{FBW}_{\text{min}} = \frac{2 \tan \theta_{\text{min}}}{(\rho_{\text{ap}}/\lambda_0) \cos \theta_{\text{min}}}. \quad (13)$$

In this regard, in Fig. 3, we have reported the metric of confinement as a contour plot of the two variables  $\theta$  and FBW for  $\rho_{\text{ap}}/\lambda_0 = 2$ . As is shown, even for such an electrically-small aperture, the conditions given by Eqs. (12) and (13) identify a region where the X-wave launcher may operate for generating X-waves that are efficiently confined along both directions. However, this would require a very large fractional bandwidth for such an electrically-small antenna (more than

20% for an aperture radius of  $2\lambda_0$ ), thus considerably limiting the class of suitable millimeter-wave devices.

#### IV. CONCLUSION

In this work, the design of efficient X-wave launchers has been discussed from an original perspective. By reviewing the concept of metric of confinement, we discussed alternative criteria for designing X-wave launchers that might be of interest for specific millimeter-wave applications. In particular, it has been shown that X-wave launchers can be designed to get either the same resolutions or the same confinement ratios along both axes. Also, we discussed the possibility to design an efficient X-wave launcher without requiring an electrically-large aperture. As is seen, this comes at the expense of a larger fractional bandwidth. The discussion outlined in this work might be beneficial in the design process of next microwave/millimeter-wave X-wave launchers. The possibility to extend these results to different class of nondiffracting waves will be envisaged in future works.

#### REFERENCES

- [1] H. E. Hernández-Figueroa, M. Zamboni-Rached, and E. Recami, *Nondiffracting Waves*, John Wiley & Sons, 2013.
- [2] D. McGloin and K. Dholakia, “Bessel beams: diffraction in a new light,” *Contemporary Physics*, vol. 46, no. 1, pp. 15–28, 2005.
- [3] J. Durnin, J. J. Miceli Jr., and J. H. Eberly, “Diffraction-free beams,” *Phys. Rev. Lett.*, vol. 58, no. 15, pp. 1499–1501, 1987.
- [4] W. Fuscaldo *et al.*, “Analysis of limited-diffractive and limited-dispersive X-waves generated by finite radial waveguides,” *J. App. Phys.*, vol. 119, no. 19, 194903, 2016.
- [5] M. Ettore, S. M. Rudolph, and A. Grbic “Generation of propagating Bessel beams using leaky-wave modes: experimental validation,” *IEEE Trans. Antennas and Propag.*, vol. 60, no. 6, pp. 2645–2653, Jun. 2012.
- [6] W. Fuscaldo, G. Valerio, A. Galli, R. Sauleau, A. Grbic, and M. Ettore, “Higher-order leaky-mode Bessel-beam launcher,” *IEEE Trans. Antennas and Propag.*, vol. 64, no. 3, pp. 904–913, Mar. 2016.
- [7] N. Chiotellis and A. Grbic, “A broadband, Bessel beam radiator,” *IEEE Int. Symp. Antennas Propag. (APS-URSI 2016)*, pp. 873–874, 2016.
- [8] S. C. Pavone, A. Mazzinghi, A. Freni, and M. Albani, “Comparison between broadband Bessel beam launchers based on either Bessel or Hankel aperture distribution for millimeter wave short pulse generation,” *Optics Express*, vol. 25, no. 16, pp. 19548–19560, Aug. 2017.
- [9] W. Fuscaldo *et al.*, “Parameterization of the nondiffractive features of electromagnetic localized pulses,” *IEEE Int. Symp. Antennas Propag. (APS-URSI 2016)*, pp. 869–870, 2016.
- [10] M. Born and E. Wolf, *Principles of Optics*, Cambridge University Press, 1997.